BCAP is a centriolar satellite protein and inhibitor of ciliogenesis.

Paul de Saram†, Anila Iqbal†, Jennifer N Murdoch and Christopher J Wilkinson.

Centre for Biomedical Sciences, Royal Holloway University of London, Egham, Surrey, TW20 0EX, United Kingdom.

Corresponding author: Christopher.Wilkinson@rhul.ac.uk
† Joint first author

Running title: BCAP is a ciliogenesis inhibitor

Keywords: centriolar satellite, cilia

Summary statement

Cilia have important roles in cell/developmental biology but little is known about what prevents cilia being made at the wrong time. We show that BCAP is an important inhibitor of ciliogenesis.

Abstract

The centrosome and cilium are organelles with important roles in microtubule organisation, cell division, cell signalling, embryogenesis, and tissue homeostasis. The two organelles are mutually exclusive. The centriole/basal body is found at the core of the centrosome (centriole) or at the base of the cilium (basal body) and changing which organelle is present in a cell requires modification to the centriole/basal body both in terms of composition and sub-cellular localisation. While many protein components required for centrosome and cilium biogenesis have been described, there are far fewer known inhibitors of ciliogenesis. Here we show that a protein called BCAP and labelled in the sequence databases as ODF2-like (ODF2L) is a ciliation inhibitor. We show that it is a centriolar satellite protein.

Furthermore, our data suggest BCAP exists as two isoforms with subtly different roles in inhibition of ciliogenesis. Both are required to prevent ciliogenesis and one additionally controls cilium length after ciliogenesis has completed.

Introduction

Cilia are hair-like structures found on the surface of many cell types and have important roles in cell signalling and embryogenesis (Nigg and Raff, 2009). Cilium defects cause inherited diseases (Badano et al., 2006), polycystic kidney disease being the most prevalent (Ong and Wheatley, 2003). Knowledge of the roles and component parts of the cilium has greatly expanded in the last decade. However, control of when a cell makes a cilium is still poorly understood.

The cilium acts a 'mast' or antenna for many signalling pathways, including hedgehog signalling (Huangfu et al., 2003). Mutations in various cilium components give rise to a large number of individually mainly rare diseases that are grouped together as the ciliopathies (Badano et al., 2006), including Meckel-Grubel, Alstrom, Joubert and Bardet-Biedl syndromes (Ansley et al., 2003; Collin et al., 2002; Dawe et al., 2007). These diseases affect multiple tissues and symptoms include retinal degeneration, polydactyly, kidney cysts and neurological features, reflecting the multiple roles of cilia in cellular communication, cellular functioning and developmental biology.

The internal frame or superstructure of the cilium is composed of an axoneme of nine microtubule doublets, cylindrically arranged (Satir and Christensen, 2007). At the base of this is another microtubule-based structure, the barrel-shaped basal body. This closely resembles the centrioles found in the centrosome, the major microtubule nucleating centre of animal cells and component of the two poles of the mitotic spindle (Bornens, 2002; Doxsey, 2001; Tassin and Bornens, 1999). Indeed, cells use a centriole to make the basal body and do so when they leave the cell cycle, either temporarily or when they differentiate into specialised cell types (Nigg and Raff, 2009).

The sequence of changes from centriole to basal body was first visualised by Sorokin using electron microscopy (Sorokin, 1962). One of the two centrioles, the mother centriole, which has additional, bracket-like

appendage structures at its distal end, acquires a vesicle-like structure at this end and migrates to the cell surface. There the membranes fuse. The basal body is tightly bound to the membrane and transition zone fibres form between the two. The axoneme is templated from the basal body and extends, covered in membrane, away from the basal body.

The switch between centriole and basal body, centrosome and cilium is tightly regulated. Autophagy is used to remove molecules that otherwise inhibit ciliogenesis (Pampliega et al., 2013; Tang et al., 2013). Few negative regulators or inhibitors of ciliogenesis are known (Kim et al., 2010). Some are components of regulatory networks that affect processes in addition to ciliogenesis (Kim et al., 2010; Kasahara et al., 2014). Others, such as OFD1 and CP110, are centrosome components (Tang et al., 2013; Tsang et al., 2008). CP110 acts through Rab8 and Cep290 to inhibit ciliogenesis (Tsang et al., 2008). It also functions to prevent microtubules extending from the distal end of the centriole/basal body (Schmidt et al., 2009). It therefore also has a role in regulating centriole and centrosome duplication during S phase of the cell cycle, when two new centrioles bud from a template assembled on the side of the two existing centrioles and gradually extend until they reach full length in early G2. OFD1 similarly is involved in regulating centriolar length and is also involved in distal appendage formation (Singla et al., 2010)

The centrosome components that are known to be negative regulators of ciliogenesis also have other roles in centrosome biology and centrosome/centriole duplication during the cell cycle. This, together with the necessarily tight control of whether a cell has a cilium versus a centrosome, suggests that dedicated, centrosome-localised inhibitors of ciliogenesis should exist. Here we report that BCAP is a negative regulator or inhibitor of ciliogenesis that needs to be removed for cilia to be made.

BCAP was first discovered by Ponsard and colleagues (Ponsard et al., 2007) but has since been annotated in the sequence databases as ODF2L or ODF2-like due to homology (28% identity, 51% similarity) to ODF2, a centriolar appendage protein (Lange and Gull, 1995; Nakagawa et al., 2001). Ponsard et al. found this protein to be expressed mainly in tissues

containing motile cilia, where its expression increased as cells differentiated and ciliated. Five isoforms were described, three long isoforms of about 65 kDa, and two short isoforms at 40 kDa. Ponsard et al. decribed BCAP as localising to basal bodies in ciliated cells and the centrioles of proliferating cells. Although there is similarity at the sequence level to ODF2, they observed that BCAP occupied a distinct zone within the centrosome.

We report here that BCAP is also a centriolar satellite protein. We detect two isoforms in our cell lines. Both inhibit ciliogenesis but appear to have subtly different roles in this process.

Results

BCAP/ODF2L/ODF2-like is a centriolar satellite protein

We previously have investigated the role of centrosome proteins in neural progenitor divisions in the zebrafish retina (Novorol et al., 2013). One protein we depleted from zebrafish embryos was ODF2, a component of the appendages of the mother centriole (Lange and Gull, 1995). Depleting this protein was not embryonic lethal but did result in various defects, including smaller eyes and brain. Since the sequence databases of mammalian species contain a sequence annotated as a related protein, ODF2-like or ODF2L, we sought to characterise this protein to see if it could be acting redundantly with ODF2. It has previously been named as BCAP (Basal body, centriole associated protein), with localisation at the basal bodies of multi-ciliated tracheal cells described (Ponsard et al., 2007).

We first tested the localisation of BCAP within human cell lines using the few commercially available antibodies and found one that gave staining near the centrosome, Biorbyt orb31049 (which we will refer to as the anti-BCAP (Biorbyt) antibody) . We expected to see localisation at one of the two centrioles only, as the centriolar appendages, of which ODF2 is part, are present on the mother but not daughter centriole (Lange and Gull, 1995; Mogensen et al., 2000; Nakagawa et al., 2001). Instead, we observed a speckled staining of numerous small punctae forming a cloud around the centrioles of the centrosome, visualized by staining for gamma tubulin (Fig. 1A-C,I).

To confirm the specificity of the staining of the anti-BCAP (Biorbyt) antibody we decided to test if it would bind to GFP-BCAP expressed in cells. HeLa cells were transfected with a plasmid encoding GFP-BCAP and then stained with anti-gamma tubulin or anti-BCAP (Biorbyt) antibody. GFP-BCAP was strongly stained by the anti-BCAP (Biorbyt) antibody we were using (Fig. 1D-F) with staining overlapping with green fluorescence from GFP-BCAP. The green fluorescence from GFP-BCAP was punctate in nature and present as a cloud around the centrosome (Fig. 1G).

This staining pattern is characteristic of centriolar satellites (Tollenaere et al., 2015), protein dense structures that are involved in transport to and from the centrosome. The prototypical centriolar satellite protein is PCM-1 (Balczon et al., 1994; Kubo et al., 1999) whose staining (Fig. 1H) resembles that of BCAP. We therefore tested if the localisation of BCAP coincided with that of PCM-1 by staining human cell lines transfected with GFP-BCAP with anti-PCM-1 antibody. There was nearly full overlap between the signals (Fig. 1J-L). This is consistent with BCAP being a centriolar satellite protein.

The structure of satellites and the localisation of many other proteins to these structures depends on the presence of PCM-1(Stowe et al., 2012). When we depleted PCM-1 by RNAi, the localisation of the BCAP signal changed. There was no centriolar satellite staining but instead a diffuse and non-punctate cytoplasmic staining was observed (Fig. 1M-O). This is again consistent with BCAP being a centriolar satellite protein.

Since some proteins have multiple localisations within the cell or within a particular organelle, such as OFD1 at the centriolar appendages and in the centriolar satellites (Ferrante et al., 2009; Singla et al., 2010; Tang et al., 2013), we carefully examined the localisation of BCAP in multiple cells. In many cells, we could observe BCAP staining around but not overlapping with that of gamma tubulin, which stains the material immediately around the centrioles (Fig. 1I).

Since BCAP has a different localisation from ODF2, we re-examined the homology between BCAP and ODF2. The two proteins only share 51% amino-acid sequence similarity and 28% identity, in a region comprising

less than half of the protein length. We then explored the relationship between ODF2 and BCAP by constructing a phylogentic tree (Fig. 2A). We compared BCAP and ODF2 sequences from animals representative of amphibians (*Xenopus tropicalis*), reptiles (*Anolis carolinensis*), birds (chicken, *Gallus gallus*), rodents (domestic mouse, *Mus musculus*) alongside the human sequences. All BCAP sequences grouped together, separate from the group of ODF2 sequences. There is a clear split between BCAP and ODF2 groups implying they diverged at the latest in the last common ancestor for terrestrial vertebrate animals. ODF2L/ODF2-like is therefore a potentially misleading name for BCAP. We will continue to use the name BCAP, as first proposed by Ponsard et al. to refer to this protein from now on. The relationship between the different isoforms of BCAP, those described by Ponsard et al. and those predicted in the NCBI database, is shown in Figure 2B, together with the binding sites of the antibodies and siRNAs used in this study, as described below.

The role of BCAP in ciliogenesis

Centriolar satellites are important for ciliogenesis and the localisation of component proteins changes during this process (Kubo et al., 1999; Stowe et al., 2012). We therefore tested the localisation of BCAP in RPE1-hTERT cells that had been induced to ciliate by serum starvation (Fig. 3). The anti-BCAP (Biorbyt) antibody showed clear satellite staining in RPE1-hTERT in serum-supplemented, proliferating conditions (Fig. 3A). However, this antibody did not stain the region around the centrioles/basal bodies in serum-starved RPE1-hTERT cells, implying that BCAP had disappeared during ciliogenesis (Fig. 3B). Whether this was by degradation or dispersal could not be determined by immunofluorescence alone. Overexpressing GFP-BCAP gave a surprising result. Staining was observed around the centrioles/basal bodies with the expected pattern but we did not observe in serum free media any transfected cells with cilia, as visualised by staining with anti-acetylated tubulin (Fig 3C,D,E). This suggested that BCAP can act to suppress the formation of cilia.

We assayed how expression levels of BCAP differed before and after ciliation. Western blotting of extracts of RPE1-hTERT and HeLa cells with the anti-BCAP (Biorbyt) antibody under serum-supplemented (non-ciliating) and serum-free (ciliating) conditions showed that BCAP was readily detectable in serum-supplemented conditions but absent when cells had ciliated (Fig. 3F,G). This suggests that during ciliogenesis existing BCAP is not dispersed from the centriolar satellites but removed from the cell.

If BCAP normally acts as a ciliogenesis inhibitor, then depleting BCAP might allow for cilia to be made under conditions in which cells normally maintain a centrosome. We depleted all isoforms of BCAP by RNAi (two separate siRNAs, locations of target sites shown in Fig. 2B). Depletion was confirmed by RT-PCR (Fig. 4A,B) and immunocytochemistry (Fig. 4C). When RPE1-hTERT cells were transfected with these siRNAs in serum-supplemented media, conditions under which they normally do not ciliate, cilia were now extensively generated (Fig. 4E,F). Cilium length was also increased by a quarter, from 3.1 μm to 4.1 μm ($p<0.001$ by ANOVA, both siRNAs) (Fig. 4G-I). This knockdown could be rescued by overexpressing mouse BCAP, whose coding sequence is not completely identical to human BCAP at the target sites of the two siRNAs used. When cells were depleted of BCAP by siRNA transfection while simultaneously transfected with an expression construct for mouse BCAP, no cilia were formed (Fig. 4K-N). Together, these overexpression and/or depletion experiments are consistent with BCAP acting as a ciliogenesis inhibitor.

Depletion of BCAP did not alter the pattern of staining of ODF2, gamma tubulin or PCM-1 (Fig. 4O-Q). Centriolar satellite and centrosome structure would therefore appear not to be grossly affected by BCAP depletion as these markers for the satellites, pericentriolar matrix and appendages showed normal localisation when BCAP was absent.

BCAP has multiple isoforms, two of which are present in RPE-hTERT cells

When we repeated these experiments with a different anti-BCAP antibody, 23887-1-AP from Proteintech (anti-BCAP (Proteintech) antibody), we obtained slightly different results. Proliferating cells still showed a satellite pattern of staining (Fig. 5A-C), but, by Western blotting, BCAP remained present though at reduced levels after ciliogenesis had completed (30% reduction, Fig. 5D,E). By immunofluorescence, in a mixed population of RPE1-hTERT cells at different stages of ciliogenesis, a portion of cells had an absence of staining and some showed satellite staining around the basal bodies (Fig. 5F-H). This staining overlapped with that of PCM-1 (Fig 5I) and partially overlapped with that of gamma-tubulin (Fig. 5J), in that centrioles as well as satellites were stained. Notably, the staining pattern was not restricted to one centriole like ODF2 (Fig 5K).

We sought to image how BCAP localization, as visualised by the anti-BCAP (Proteintech) antibody, changes during ciliogenesis. We synchronised cells with a nocodazole block, then released them into medium lacking serum and fixed samples every hour. These samples were then stained with the anti-BCAP (Proteintech) antibody (Fig. 6A) and acetylated tubulin antibody.

BCAP staining changed during the course of ciliogenesis. Immediately after release from the nocodoazole block, BCAP staining showed a scattered pattern (Fig. 6A). BCAP then adopted a more satellite-like appearance within an hour. As ciliogenesis started, all BCAP staining disappeared, with negligible fluorescence signal (Fig. 6B). As ciliogenesis neared completion at 8h (Fig. 6C), BCAP staining was then again observed in the centriolar satellites (Fig. 6A) with BCAP returning to 50% of pre-ciliogenesis levels (Fig 6B).

The different results from the two anti-BCAP antibodies used could be explained by the existence of multiple isoforms of BCAP. ENSEMBL and NCBI databases predict several splice variants of BCAP based on genomic and EST data (Fig 2B), and Ponsard et al. (2007) describe five isoforms. We have combined these data in Figure 2B, using Greek letters to label the combined set, but also showing the names used by Ponsard et al. and the NCBI database, on the right-hand side of the figure,. There are five long

isoforms, all of similar size, which vary by the inclusion of exons 2, 10, 13 and 14, plus two short isoforms that include exon 10 but differ by the presence/absence of exons 13 and 14.

We tested RPE-hTERT cells for the presence of these isoforms by RT-PCR. With the primer pair used to test for inclusion/skipping of exon 10, we observed only the smaller band produced if exon 10 was skipped (Fig 7A). This is consistent with the short isoforms and two of the long isoforms being absent, isoforms β, γ, ζ, η. For exon 13, we observed both larger and smaller bands which would be produced if this exon was either included or skipped in different isoforms. These data are consistent with the presence of the α, δ and ε isoforms (Fig. 2B). When we cloned and sequenced BCAPδ/ε, we observed only the δ isoform (Fig. 7B), and similarly, we observed only one band when amplifying BCAPα. In our cells, it would appear that only the α and δ isoforms are present. Compared to BCAPα, in BCAPδ exon 13 is skipped but exon 19 substitutes for the very short exon 18 that is incorporated in BCAPα. BCAPα and δ will therefore have almost identical molecular masses of 69kDa.

The anti-BCAP (Biorbyt) antibody was raised to the C-terminus of BCAPα whereas the anti-BCAP (Proteintech) antibody was raised to the common N-terminus of both α and δ isoforms (Fig. 2B). The results above suggest that in RPE-hTERT cells two isoforms of BCAP exist with slightly different expression patterns. BCAPα is completely removed in ciliated cells. BCAPδ returns to cells that have made cilia.

To further refine the roles of the two variants, we cloned the human BCAPα and BCAPδ. GFP-BCAPα showed centriolar satellite staining and no centriolar staining (Fig 7C-K) consistent with the antibody staining. In contrast, GFP-BCAPδ showed centriolar and satellite staining (Fig 7L-Q). The antibody to all isoforms (α to η) of BCAP, raised by Ponsard et al. (2007), stained centrosomes, centrioles and basal bodies in human nasal epithelial (HNE) cells.

We depleted each isoform separately. By RT-PCR, depletion was 89% and 80% respectively for BCAPα and BCAPδ (Fig. 8A,B). In both cases, the

anti-BCAP (Proteintech) antibody staining decreased but was not eliminated, consistent with it binding both isoforms (Fig 8 C-E). Depletion of either protein using a variant-specific siRNA resulted in ciliogenesis occurring in serum-supplemented conditions. 30% of cells now formed cilia when either BCAPα or BCAPδ was depleted alone, compared to 70% when both isoforms were depleted together (Fig 8F). This is consistent with the two isoforms acting together to suppress ciliation.

When either BCAPα or BCAPδ were depleted from cells undergoing serum starvation, cilia were formed as expected but it was notable that cilium length increased in BCAPδ depleted cells but not in those depleted of BCAPα (Fig 8G-J).

Overexpression of either GFP-BCAPα or GFP-BCAPδ suppressed cilium formation in serum-free media, consistent with our previous observations (Fig 8K-P). The proportion of cells with cilia decreased from 80% to 25% in both cases (Fig 8Q). There appears to be partial redundancy in the roles of BCAPα and BCAPδ since overexpressing BCAPα in cells depleted of BCAPδ suppresses ciliation and the reciprocal experiment yields the same result (Fig. 8R-X).

These data suggest that BCAP exists as two isoforms in RPE1-hTERT cells. Both isoforms are removed during ciliogenesis but one, BCAPδ, reappears once ciliogenesis has completed. Both suppress ciliation but additionally BCAPδ acts to control cilium length once cilia have formed.

BCAP depletion does not affect a role in microtubule regrowth and reorganization nor the cell cycle

Since other ciliogenesis inhibitors, OFD1 and CP110 have additional centrosome/centiole-based functions (Schmidt et al., 2009; Singla et al., 2010), we assayed BCAP for other roles at the centrosome. We first tested if BCAP had a role in microtubule nucleation, a major role of the centrosome in interphase cells (Bornens, 2002; Tassin and Bornens, 1999), using the microtubule regrowth assay (Fry et al., 1998). BCAP-depleted cells (both

isoforms; siRNA1) showed no detectable difference in the time at which microtubule nucleation restarted or the rate at which the network was re-established, compared to control treated cells (Fig. S1A-J). BCAPα and δ are therefore not required for microtubule nucleation. At the zero time-point, the microtubule network in BCAP-depleted cells appeared similar to that of control cells so the mature microtubule network seems unaffected by removal of BCAPα/δ.

We also tested whether BCAP is required for adjusting an existing microtubule network. We used the wound assay on confluent RPE1-hTERT cells to test if BCAP (either isoform) had a role in cell migration and polarity through the centrosome (Nobes and Hall, 1999)(Luxton and Gundersen, 2011). In both control and siRNA-transfected cells, the wound closed at the same rate (Fig. S1K-P). Staining the cells for Golgin-97 and gamma tubulin showed that both BCAP-depleted and control cells behaved the same, with the Golgi apparatus and centrosome reorientating towards the direction of the wound during closure (Fig. S1Q,R). By this assay, depletion of BCAP (both isoforms) neither inhibits migration nor adversely affects cell polarity.

Finally, we tested for a role of BCAP in the cell cycle. The centrosome contributes to the poles of the mitotic spindle and has a critical role both in nucleating astral microtubules and facilitating the fast generation of a mitotic spindle (Basto et al., 2006; Stevens et al., 2007). Furthermore, depletion of many centrosome proteins results in a G1 arrest, before the cells commit to entering the cell cycle (Mikule et al. 2007). We found that BCAP-depleted RPE1-hTERT cells showed the same distribution of cell cycle phases as control treated cells, after 24 h culture (Fig. S2A,B), including after first serum-starving the cells for 24 h (Fig. S2C, D). Thus BCAP depletion (both isoforms) does not cause a G1 block nor does it prevent progression into mitosis. On balance, the role of BCAP appears to be specific to the regulation of ciliogenesis.

Discussion

We describe here BCAP as a centriolar satellite protein that acts as an inhibitor of ciliation, specifically, the initiation of ciliogenesis. Overexpression of BCAP in cells, under conditions that normally cause cells to form cilia, prevents this from occurring. Depletion of BCAP under conditions in which ciliation is not normally observed results in a substantial portion of cells producing cilia.

Many centrosome proteins, including those in the satellites, have been shown to contribute to ciliogenesis. Few proteins, centrosomal or otherwise, have been found to be inhibitors of ciliation. BCAP partially resembles OFD1, a known inhibitor of ciliogenesis in that depletion of OFD1 modulates ciliogenesis in the same direction and with the same magnitude as depletion of BCAP (Tang et al., 2013). Whereas OFD1 has other roles in centrosome biology, so far we have not been able to determine other roles for BCAP in centrosome function. BCAPα appears to be present at centriolar satellites only in cycling cells with BCAPδ at the centrioles in addition; OFD1 is also present at the appendages (Singla et al., 2010). While super-resolution or immuno-gold TEM would categorically rule out other localisations, we do not observe any BCAPα at the centrioles in cycling cells, although we do observe BCAPδ at both the centrioles in addition to satellite staining.

The antibody raised by Ponsard et al. was designed to detect all BCAP isoforms, using a mixture of peptide sequences encoded by exons 13 and 15. Exon 15 is included in all isoforms, although exon 13 is present in only two of the long isoforms (L-BCAP/α and L-BCAP del 2/ε), and one short isoform (S-BCAP/η). Ponsard et al. also used human nasal epithelial (HNE) cells in an air-liquid interface culture to cause differentiation of the cells into multi-ciliated epithelial cells. Both the peptide against which the antibody was raised and the nature of the cell line used may contribute to the centrosome/centriole staining they observe, which resembles the staining we observe in some cells when GFP-BCAPδ is expressed in RPE-hTERT cells.

Another ciliation inhibitor, CP110, localises to the distal tips of centrioles to act as a capping protein (Schmidt et al., 2009). In this role, CP110 can control elongation of the pro-centrioles during centriole

duplication in S-phase. BCAPα does not show centriolar localisation but BCAPδ does to some extent. During ciliogenesis, CP110 acts through Rab8 and Cep290 to control ciliation initiation (Tsang et al., 2008). Cep290 is another satellite protein. Whether BCAPα and/or δ link CP110 and Cep290 together or inhibit ciliogenesis by a different means would be a logical avenue for future investigation.

Any explanation of how BCAP controls ciliogenesis also has to consider the seven possible splice variants predicted by us and others. Our analysis in RPE-hTERT cells supports the presence of two protein isoforms, with only one detected by the anti-BCAP (Biorbyt) antibody but both detected by the Proteintech antibody. The BCAPα variant detected by the anti-BCAP (Biorbyt) antibody completely dissappears during ciliogenesis, implying its removal is required for ciliogenesis to initiate, continue and for cilia to be maintained. The anti-BCAP (Proteintech) antibody shows that total BCAP, 'α' and 'δ' variants together, disappears at the start of ciliogenesis but BCAP returns, albeit at a lower levels, once ciliogenesis is complete. This can be explained if the 'δ' variant also needs to be removed for ciliogenesis to start and then the 'δ' form has another function once cilia have been made. BCAP α and δ are partially redundant in that both can suppress ciliation but removal of either one by RNAi only gives half the rate of ciliation observed when both are removed at the same time. In HNE cells, which differentiate into multi-ciliated (motile) cells, as opposed to monociliated (immotile) RPE-hTERT cells, more isoforms may be needed to ensure this process is properly controlled. An added complication in multi-ciliated cells is the requirement for centriole duplication to generate the (hundreds of) extra basal bodies, ciliogenesis from which then needs to be controlled and directed to the correct side of the cell.

We tested several other centrosome functions in BCAP depleted cells as the siRNAs used for RNAi-mediated depletion target a region shared by both variants. Depletion of total BCAP, both α and δ variants, did not affect microtubule regrowth, cell polarity, migration or re-entry into the cell cycle.

Instead, the function of BCAPδ could be regulation of cilium length. In cells transfected with siRNA duplexes targetting both BCAP variants, cilium length is increased. Depletion of BCAPδ also results in an increase in cilium length but this is not observed when BCAPα is depleted. BCAPδ may therefore additionally act as a late inhibitor of ciliogenesis, moderating cilium length. There are therefore parallels and contrasts to the roles ascribed in ciliogenesis to autophagy. In this regard it is of note that BCAP is predicted to have an APG6 domain (region similar to yeast autophagy protein 6).

Early on after serum starvation and initiation of ciliogenesis, autophagy is activated and Tang et al. (2013) show that this is needed to remove OFD1, an inhibitor. Pampliega et al. (2013) further show that autophagy needs to be directed differently before, during and after ciliogenesis. Once ciliation has finished, and full-length cilia have been made, autophagy is directed to limiting cilium length. In this situation, reduced autophagy results in abnormally long cilia. The latter mirrors the effect of absence of BCAP in cells in which cilia have been established. Autophagy and BCAP would therefore both appear to have a role at this stage in limiting cilium length. Pampliega et al. (2013) propose that in unciliated cells and those which possess cilia, autophagy is used to limit the availability of IFT20 which it turn affects Golgi-cilium movement. BCAP might therefore aid in this process. However, when ciliogenesis initiates, BCAP needs to be removed. It is not clear then if BCAP is a target of autophagy, like OFD1, or an aid in the pathway. The presence of two distinct isoforms may be due to this requirement to have BCAP present before and after ciliogenesis but not during the process.

BCAP has also been shown to be upregulated in the mouse trachael cell ciliation model, (Vladar and Stearns, 2007) though the data do not show which variant (Tim Stearns, personal communication). If BCAPδ is required to moderate cilium length, then it would be consistent that its expression is upregulated in cells with hundreds of cilia, as opposed to the one primary cilium in the cell lines studied here.

Future work will be to place BCAP within known ciliogenesis regulatory networks, inhibitory mechanisms and processes that relieve this repression. Obvious processes to check are the autophagy pathway and IFT20-mediated control of primary ciliary vesicle formation. The CP110/Cep97/Cep290 pathway could be checked as well, though the current localisation data point away from this mechanism. These hypotheses will form the basis of more extensive future studies.

Materials and methods

Cell culture

HeLa cells were provided by Prof. George Dickson's laboratory at Royal Holloway. The hTERT-immortalised human retinal pigment epithelial cell line (RPE1-hTERT, ATCC cat#: CRL-4000) was kindly provided by Prof. Erich Nigg, Basel, Switzerland. HeLa cells were grown in Dulbecco's Modified Eagle's Medium (Sigma D6546) supplemented with 2 mM L-Glutamine (Sigma G7513), 10% Foetal Bovine Serum (Gibco 10500-064) and 1% antibiotic-antimycotic mixture (Gibco 15140-122). hTERT-RPE-1 cells were grown Dulbecco's Modified Eagle's Medium with nutrient mixture F-12 Ham (Sigma D6421) supplemented with 10% Foetal Bovine Serum, 0.348% sodium bicarbonate and 1% antibiotic-antimycotic mixture. HuH-7 cells were cultured in Dulbecco's Modified Eagle's Medium (Sigma D6546) supplemented with 10% Foetal Bovine Serum and 1% antibiotic-antimycotic mixture. Cells were grown in Corning 25 and 75 cm^2 vent-capped flasks and 6-well plates (Nunc, Denmark) and incubated at 37°C with 5% CO_2 in a humidified incubator and confluence was assessed by microscopy. Ethanol-washed coverslips were added to the 6-well plates to enable subsequent processing for immunofluorescence microscopy. These coverslips were fixed in methanol at -20°C or 4% (v/v) formaldehyde (FA) for 3-5 min before antibody incubation.

Immunocytochemistry.

Coverslips were blocked in 1% or 3% BSA in PBS for 30 min at room temperature. After blocking, coverslips were placed on top of a paraffin film attached to flat surface. Then 100-200 µL of primary antibody solution was added to the top of the coverslip. The coverslip were incubated with the primary antibody for 60-120 min at room temperature or overnight at 4°C. After the incubation, coverslips were transferred back to a 6-well plate and washed three times with PBS at room temperature. Then the coverslips were incubated with the secondary antibodies identically to the procedure described above and incubated for 60 min at room temperature. After the incubation, coverslips were transferred back to a 6-well plate and washed again with PBS three times and then mounted on 10-15 µL of Vectashield mounting media with DAPI (Vectorlabs, Peteborough, UK) on to glass slides for microscopy. The mounted coverslips were sealed with nail varnish and left to dry for 1-2 hours in a dark chamber before microscopy. Primary antibodies used as follows: mouse acetylated α-tubulin (Sigma-Aldrich, T7451) 1:500; Mouse anti-γ-Tubulin (Sigma-Aldrich, T6557) 1:2500; mouse anti-PCM1 1:1000 (CL0206, Sigma); Rabbit anti-γ-Tubulin (Sigma-Aldrich, T5192) 1:1000; Mouse anti-Golgin-97 (ThermoFisher, Q92805) 1:1000; Rabbit Anti- BCAP (Biorbyt, orb31049) 1:100; Rabbit anti- BCAP (Proteintech, 23887-1-AP); and Rabbit Anti-PCM-1 (Sigma, HPA23374), 1:1000. Secondary antibodies used as follows: Anti-mouse Alexa Fluor 594 (Invitrogen) 1:1000 and anti-rabbit Alexa Fluor 488 1:1000.

Images collected with either Nikon Eclipse TE300 inverted microscope (Nikon, UK) with 40x Plan Flour objective (Nikon) or 60X Plan Apochromat oil immersion objective with NA 1.4 standard filter sets (Nikon) attached to 1.3 megapixel ORCA-100 cooled CCD camera (model C4742-95, Hamamatsu, Japan) and Hamamatsu HCImageLive (Hamamatsu Corporation, Japan) software or Nikon Eclipse Ni-E microscope (CF160 optical system, Nikon) with 60X Plan Apochromat oil immersion objective attached to 1.5 megapixel monochrome DS-Qi1MC cooled CCD camera and NIE Br (Nikon, UK) software. Confocal microscopy stacks were obtained with the Olympus IX81/FV-1000 laser confocal system with 63X Plan Apochromat oil immersion objective (Olympus) using Ar gas laser and He-Ne

diode laser. Image Z-stacks were analysed using Olympus FV-1000 Fluoview 2.0 C software.

Molecular cloning and transient transfection of DNA into Mammalian cells.

Molecular cloning followed standard protocols (Sambrook and Russell, 2001) and the instructions of the manufacturer of the kits, reagents and enzymes used. All restriction enzymes and polymerases were obtained from Promega (UK). The mouse full length BCAP cDNA I.M.A.G.E clone (cDNA clone MGC: 28123, IMAGE:3979963, Gene bank accession BC020075.1, Gene ID 52184) was purchased from Source BioScience (Nottingham, UK). The mouse cDNA was amplified and 5' *Bam*H I and 3' *Xho* I restriction sites were added to the cDNA during amplification by PCR using (5' ttttggatcctcATGGAGATGCCTACTAGTGATGG 3' and 5' ttttctcgagttagtcgacTCTAAACATCGTTACATAGGAAATTTG 3'). Then a *Bam*H I-*Xho* I fragment containing full-length BCAP was inserted into the pCS2P+EGFPN cut with *Xho* I and *Bgl* II. Similarly we cloned hBCAPα and hBCAPδ using primers 5' tttgggatcctgATGGAGAAGGCTGTAAATGA 3' (Forward primer for both transcripts), 5' tttgtcgacTCATGGAGTCTCTGGATCAC 3' (reverse primer hBCAPα) and 5' tttgtcgacTTATTCAAACATTGTTACATAA 3' (reverse primer hBCAPδ). The PCR product was cut with *Bam*H I- *Sal*1, and inserted into pCS2P+EGFPN cut with *Sal*1- *Bgl* II.

HeLa and RPE1-hTERT cells were transiently transfected with DNA constructs for expression using Lipofectamine 2000 (Life Technologies) according to the manufacturer's protocols. For all the transfections in 6-well format, 2.5 – 3 µg of plasmid DNA was used and diluted in 250 µL Opti-MEM. Both, Lipofactamine 2000 and DNA mixtures were incubated for 5-10 min at room temperature before combining together and then addeing to each well and incubating for 5-6 h (37°C with 5% CO_2) before replacing with serum supplemented, antibiotic free medium and incubating for 24-48h.

RNA interference

The siRNAs were designed with custom RNA synthesis tools (siDESIGN Center) provided by GE Dharmacon to BCAP transcripts: XM_005271056, NM_001184766, NM_020729, XM_005271057, NM_001184765, NM_001007022, XM_005271055, XM_005271054. The siRNA oligo sequences were designed to have overlap of 19 nucleotides and 2 nucleotide overhangs on both 3'-end of the sense and anti-sense strands. Following siRNAs were used for the experiments; Hs*BCAP* siRNA1 GCAAGAAGCAGCUGAAAUAUU (sense)/GCAAGAAGCAGCUGAAAUAUU (antisense) and Hs*BCAP* siRNA2, GGAGAAGGCUGUAAAUGAUUU (sense)/ AUCAUUUACAGCCUUCUCCUU (antisense). The siRNA sequences targeting the two individual transcripts Hs*BCAP*α siRNA UGAAGGAGUUAGAGCGUGUUU (sense) / ACACGCUCUAACUCCUUCAUU (antisense) and Hs*BCAP* δ siRNA AGUCUUGAGAAGUCGGAAAUU (sense)/ UUUCCGACUUCUCAAGACUUU (antisense). A SMARTPool ON-TARGETplus siRNA to PCM-1 was purchased from Dharmacon. Oligos were resuspended in 200 µL of RNase-free water to make a stock solution of 100 µM and stored at -80°C. The working concentrations of 10 µM aliquots were also made by diluting 100 µM stock with RNase free water and stored in -80°C. For delivering siRNAs to mammalian cells, Lipofectamine RNAiMAX (Life Technologies) was used according to manufacturer's protocol. For transfection of mammalian cell lines, $1x10^6$ cells were plated per well of a 6-well plate (reverse transfection). All the transfection complexes were prepared in sterile 6-well plates and for each well, 2.5-3 µL of siRNA (from 10 µM working concentration) and 7.5 µL of Lipofectamine RNAiMAX diluted in 500 µL of Opti-MEM and mixtures were incubated at room temperature for 10-15 min to allow the complexes to form. Then the cell suspension was added to each well containing siRNA-RNAiMAX complexes and diluted with culture medium without antibiotics to make a final volume of 2.5 mL per well.

Cell extracts, SDS PAGE and Western blotting

Whole-cell extracts for Western blotting were prepared by washing cells in phosphate-buffered saline (PBS), followed by lysis in cell lysis buffer (50 mM Tris-HCL (pH 7.5), 150mM NaCl, 1 mM EDTA, 10% Glycerol, 1% Triton X-100) containing a protease inhibitor cocktail (P8340, Sigma-Aldrich) at 4°C for 30 min. Then the cell debris was removed by centrifuging at 12000 xg at 4°C for 20 min. Prior to SDS-PAGE, protein concentration was determined using BioRad DC assay (BioRad, UK) according to the manufacturer's instructions. Small 10% SDS polyacrylamide gels (8x6.5x cm) with 0.75mm thickness were hand cast using Biorad Mini-Protein II casting chamber. Approximately 5-15 µg of protein samples were prepared with 1x SDS-PAGE buffer and 1x reducing agent (Invitrogen), heat denatured for 10 min at 70°C and kept in ice until loaded. For running the gel, 20 µL of the protein sample alone with PageRuler Plus pre-stained protein ladder (ThermoFisher Scientific) were loaded in to each well and gels were run with SDS-PAGE running buffer (Sambrook and Russell, 2001) in a BioRad Mini Protein II gel chamber at 100 V for 1.5 h. The proteins separated from SDS-PAGE gel subsequently transferred on to activated PVDF-FL (Millipore) membrane with an aid of BioRad mini protein II wet blotting system filled with transfer buffer. Membranes were blocked with Odyssey blocking solution (Licor) or 1x Casein buffer (Sigma-Aldrich, B6429), and washed with Tris-buffered saline containing 0.5% Tween20 (Sigma-Aldrich) and probed with primary antibodies. Bound primary antibodies were detected using secondary antibodies (anti-mouse IRDye 680RD, 1:15000 and anti-rabbit IRDye 800CW, 1:15000) using Odyssey SA near infrared fluorescent (Licor) detector. The images were captured using Image studio software (Licor) version 3.

Cells migration assay (Scratch-Wound Assay)

To assess the cell migration pattern and polarity, a scratch-wound assay was performed on RPE1-hTERTcells. The cells were seeded on to a glass coverslip placed in a 6-well plate and grown in an incubator to reach

about 90% confluency. Then a linear scratch wound was made using a blunt sterile P200 tip between parallel edges of the coverslip as described in (Wells and Parsons, 2011; Nobes and Hall, 1999). The coverslips were washed two times with PBS and incubated with fresh media for 24h until the wound was closed. The coverslips were fixed in cold methanol at different time points before processing for immunocytochemistry as above.

Cell cycle synchronisation

For cell synchronisation at G2/M transition phase, hTERT-RPE1 cells were seeded and cultured until 70-80% confluency followed by treatment with 1.5 µM nocodozole for 24h as described (Uetake and Sluder, 2007). To release from G2/M arrest, cells were washed twice with PBS and incubated in serum free growth media. Cells were fixed at various timepoints in 1% FA and stained with anti-γ-tubulin, anti-BCAP and anti-acetylated alpha tubulin primary antibodies as above.

Cells cycle analysis using FACS

For the FACS based cell cycle analysis, hTERT-RPE-1 cells were grown under normal culture conditions in a 6-well plate. Once the cells reached 80-90% confluency, cells were trypsinised and harvested as described above and washed twice with PBS. The cells were then fixed in ice cold 70% ethanol for at least 30 min on ice and washed twice with PBS. Cells were treated with 100 µg/ml RNase A solution in PBS followed by 50 µg/ml propidium iodide (PI). Cells were stained overnight in a dark chamber at room temperature and data was collected using BD FACSCANTO I (BD Bioscience, Oxford, UK) flow cytometer set to collect in the linear scale. Cell cycle analysis was performed using BD FACSDiva (BD Bioscience) and FlowJo version X.

Phylogenetic analysis

Data was aligned and trees were constructed in CLC genomics workbench v7.5, using the default settings for alignment (Gap open cost 10, Gap extension cost 1) and with trees estimated using Kimura protein distances, with neighbour joining.

Acknowledgements

We would like to thank Simona Ursu for technical support. We thank Prof. Ian Barnes and Dr Selina Brace (NHM, London) for their assistance in generating the phylogenetic tree.

Competing interests

We have no competing interests.

Author contributions

PdS and AI performed the experiments and prepared the figures. CJW wrote the manuscript with help from JNM.

Funding

This research did not receive any grant from any funding agency in the public, commercial or not-for-profit sectors.

Figure Legends

Figure 1. Localisation of ODF2-like / BCAP. A-C) HeLa cells stained with anti-γ-tubulin (A, red), the anti-BCAP (Biorbyt) antibody (B, green) and DAPI (blue in combined image, C) showing a cloud of small spots clustered around the centrosome, 1-2 punctae of γ-tubulin. D-F) anti-BCAP staining (red, D) coincides with GFP-BCAP fluorescence (green, E), the overlaid signals shown in (F). G) GFP-BCAP (green) displays a punctate staining

around the centrosome, cells stained with anti-gamma tubulin (red), DAPI in blue. H) HeLa cells stained with anti-PCM1 antibody (green) show a similar pattern of staining, characteristic of centriolar satellites. I) For BCAP (green), staining is around the centrosome but not on the centrioles: γ-tubulin (red) staining does not overlap with BCAP. This is a magnified portion of (C). J-L) PCM-1 staining (red, J) coincides with GFP-BCAP staining (green, K), the overlaid signals shown in (L). M) PCM1(green), γ-tubulin (red) are unaffected in control siRNA cells. N) PCM-1 (green) is depleted by RNAi using an siRNA targetted to PCM-1 (γ-tubulin in red). O) siRNA depletion of PCM-1 results in BCAP (green) no longer localising at the satellites. Instead a diffuse, non-punctate cytoplasmic staining is observed. Scale bars 10 μm except (E), 2 μm.

Figure 2.

A) Phylogenetic analysis of the relationship between BCAP and ODF2. Sequences used were from *Xenopus tropicalis* (Xt), *Anolis carolinensis* (Ac), *Gallus gallus* (Gg), *Mus musculus* (Mm) and *Homo sapiens* (Hs). The tree was constructed using CLC Genomics. Bootstrap support values are indicated above branches. B) Schematic of the BCAP gene and BCAP isoforms. The NCBI database and Ponsard et al. have predicted/observed several transcripts and isoforms. These are summarised here. We have named them α–η to combine while avoiding confusion. NCBI numbering (a-d) and Ponsard et al. naming schemes (S/L-BCAP del x) are also shown for completeness. In isoforms where exons are skipped, the number of the exon skipped is in the gap between the two exons that are incorporated. Single-headed arrows show the binding sites for primers used to determine which variants were present. Target sites for the siRNAs used in this study are shown in red at the base of the diagram, lines with blunt arrowheads showing which isoforms would be targetted. The α and δ protein isoforms differ in the C-terminus, with BCAPα having a 50 amino acid insertion by inclusion of exon 13 compared to BCAPδ, which possesses an additional 20 amino acids in the tail due to inclusion of exon 19 instead of exon 18. The

anti-BCAP (Biorbyt) antibody was raised to the C-terminus of BCAPα whereas the anti-BCAP (Proteintech) antibody binds the N-terminus of BCAP and so will detect both BCAPα and BCAPδ.

Figure 3. BCAP and ciliogenesis. A) In proliferating RPE1-hTERT cells in serum-supplemented medium (SSM), endogenous BCAP (anti-BCAP (Biorbyt) antibody, green) localises in satellites around the centrosome (γ-tubulin, red) next to the nucleus (DAPI, blue). B) In serum-free medium (SFM), cilia (acetylated tubulin, red) are formed and BCAP staining (green) disappears (DAPI in blue). C, D) When cells are transfected with a GFP-BCAP expression plasmid (C, GFP only; D, GFP plus acetylated tubulin (red) and DAPI (blue)), untransfected cells (left-hand cell) form a cilium whereas transfected cells do not (right-hand cell). E) There is a 40% reduction in the number of cells with cilia when GFP-BCAP is expressed ($p<0.001$ by Student's t-test, 100 cells counted , n=3). G) Western blotting confirms that BCAP (green, running at nearly 70kDa), does not disperse, instead the protein disappears. This is quantified in (F).

Figure 4. BCAP depletion promotes ciliogenesis. A, B) two different siRNA duplexes both effectively deplete BCAP: a 600 bp fragment of *BCAP* is amplified by RT-PCR in various control samples (untransfected, lipofectamine and non-target siRNA) but is absent when proliferating RPE1-hTERT cells are treated with the siRNAs; beta actin is amplified to the same level in all samples (three independent experiments $p<0.001$ by one-way ANOVA). C) By immunofluorescence, BCAP signal disappears in siRNA-treated cells (BCAP signal alone in green). D) γ-tubulin signal is unaffected by BCAP depletion (γ-tubulin in red, BCAP in green, plus DAPI in blue). E) A large portion of these cells in serum supplemented medium now form cilia (acetylated tubulin in red) F) Only 7% of control cells form cilia but 79% of cells treated with siRNAs ciliate, total of 100 cells counted, $p<0.001$ by chi-squared. This is data from one experiment; three repeats show similar results. G-I) Cilium length also increases in serum-starved and BCAP-depleted RPE1-hTERT cells from 3 μm to 4 μm, $p<0.001$ by Student's t-test,

150 cilia counted in each sample. (J). Examples of control cilia are shown in (G), long cilia observed after siRNA treatement shown in (H) and (I). K-N) Mouse BCAP will rescue RNAi-depletion, with transfected cells not making cilia, shown separately in (L) and with DAPI and GFP-BCAP together in (M) ($p<0.001$ by Student's t-test, 100 cells counted in three separate repeats) . BCAP staining is much reduced in BCAP siRNA treated cells (O-Q). However, γ-tubulin (P) and PCM-1 (Q) staining are unaffected.

Figure 5. BCAP consists of at least two isoforms. A-C) in proliferating RPE1-hTERT cells in serum supplemented medium (SSM), the anti-BCAP (Proteintech) antibody (green) shows satellite staining around the centrosomes (γ-tubulin, red). D,E) in contrast to the Western blot using the Biorbyt antibody as probe, when the anti-BCAP (Proteintech) antibody (green) is used to probe cell extracts before and after ciliogenesis, levels of this protein decrease slightly rather than disappear. Beta actin is stained in red. F-H) In serum free medium (SFM), cells at presumably different stages of ciliogenesis can be observed. BCAP can be observed at the base of the cilium or clustered away from it. I) The anti-BCAP (Proteintech) antibody staining (green) colocalises with that of PCM-1 (red). J) Satellite-like staining of BCAP from the anti-BCAP (Proteintech) antibody (green) but with some overlap with the γ-tubulin signal (red). K) As expected, ODF2 (red) shows a single punctum of signal (the mother centriole) in contrast to the staining from the anti-BCAP (Proteintech) antibody (green). Scale bar, 10 μm.

Figure 6. BCAP levels and localisation change during ciliogenesis. RPE1-hTERT cells were synchronised by a nocodazole block followed by release. Samples were fixed at hourly intervals, with timepoints at which key changes took place shown here. After release at 1h, BCAP (green) is dispersed in the cytoplasm, as is the γ-tubulin signal (red). While the γ-tubulin signal reorganises into recognisable centrosomes between 2-4h, BCAP signal disappears. At 6h, cilia are visible and BCAP signal is returning. By 8h, ciliogenesis appears complete and strong BCAP signal is visible at the base of cilia. Cells were also stained with DAPI (blue). The right

hand column summarises these changes, with satellites/BCAP as small green dots, the centrioles/basal body/cilium in red and nucleus in blue. B) Signal intensity of BCAP was measured at each stage. BCAP is highly expressed at the first time-point and then gradually decreases. By 8 hours its expression has increased again to 50% of its pre-ciliation value. C) Number of cilia at each time point was measured, with 60% of cells showing cilia by 8h. This represents three independent experiments. Scale bar, 10 μm.

Figure 7 BCAP exists as multiple isofroms, two are present in RPE1-hTERT cells. A) RT-PCR using primers to amplify exons 9-11 yields one smaller band corresponding to skipping of exon 10. RT-PCR with primers to amplify exons 12-15 yields two bands corresponding to inclusion or skipping of exon 13. B) Full-length BCAPα and δ are present in RPE1-hTERT cells. There is only one band for BCAPδ but the primers would also amplify the shorter BCAPε were it to be present. C-E) GFP-BCAPα shows a satellite-like staining that colocalises with that of PCM-1 (red). F-H) This GFP-BCAPα signal is around but not overlapping γ-tubulin (red). I-K) GFP-BCAPα forms a cloud of punctae around the single ODF2 punctum (red). L-N) GFP-BCAPδ shows a pericentriolar/centriolar-like staining, overlapping γ-tubulin in about 80% of cells. O-Q) GFP-BCAPδ shows a satellite-like staining overlapping PCM-1 (red) in about 20% of cells.

Figure 8 BCAPα and δ have overlapping but subtly distinct roles in ciliogenesis. A-B) BCAPα and BCAPδ were depleted individually by siRNA. The amount of depletion of each isoform was assessed quantitatively by RT-PCR ($p<0.001$ by one-way ANOVA, three repeats). C-E) Depletion of either BCAPα or δ individually reduces but does not eliminate the Proteintech antibody staining (green) which binds both isoforms. γ-tubulin staining (red) shows the centrioles and pericentriolar matrix are grossly intact. F) Depletion of either isoform, BCAPα or δ, individually causes cells to form cilia in serum supplemented conditions ($p<0.001$ by one-way ANOVA, 100

cells counted in three repeats). G-I) In BCAPδ– but not BCAPα– depleted cells longer cilia are observed, quantified in (J) ($p<0.001$ by one-way ANOVA, 100 cells counted in three repeats). K-P) Expressing either GFP-BCAPα or δ in serum-free conditions suppresses normal ciliation. Left hand cell is untransfected, right hand cell is transfected. Cilia labelled with anti-acetylated tubulin (red). This is quantified in (Q) ($p<0.001$ by one-way ANOVA, 100 cells counted in three repeats). R-X) GFP-BCAPα can rescue BCAPδ-siRNA, with cells not making cilia in serum-supplemented conditions (cilia / acetylated tubulin in red). The same is true for the reciprocal experiment. This is quantified in (X) ($p<0.001$ by one-way ANOVA, 100 cells counted in three repeats).

References

Ansley, S. J., et al. 2003. Basal body dysfunction is a likely cause of pleiotropic Bardet-Biedl syndrome. *Nature,* 425**,** 628-33.

Badano, J. L., Mitsuma, N., Beales, P. L. & Katsanis, N. 2006. The Ciliopathies: An Emerging Class of Human Genetic Disorders. *Annu Rev Genomics Hum Genet,* 7**,** 125-148.

Balczon, R., Bao, L. & Zimmer, W. E. 1994. PCM-1, A 228-kD centrosome autoantigen with a distinct cell cycle distribution. *J Cell Biol,* 124**,** 783-93.

Basto, R., Lau, J., Vinogradova, T., Gardiol, A., Woods, C. G., Khodjakov, A. & Raff, J. W. 2006. Flies without centrioles. *Cell,* 125**,** 1375-86.

Bornens, M. 2002. Centrosome composition and microtubule anchoring mechanisms. *Curr Opin Cell Biol,* 14**,** 25-34.

Collin, G. B., et al. 2002. Mutations in ALMS1 cause obesity, type 2 diabetes and neurosensory degeneration in Alstrom syndrome. *Nat Genet,* 31**,** 74-8.

Dawe, H. R., et al. 2007. The Meckel-Gruber Syndrome proteins MKS1 and meckelin interact and are required for primary cilium formation. *Hum Mol Genet,* 16**,** 173-86.

Doxsey, S. 2001. Re-evaluating centrosome function. *Nat Rev Mol Cell Biol,* 2**,** 688-98.

Ferrante, M. I., Romio, L., Castro, S., Collins, J. E., Goulding, D. A., Stemple, D. L., Woolf, A. S. & Wilson, S. W. 2009. Convergent extension movements and ciliary function are mediated by ofd1, a zebrafish orthologue of the human oral-facial-digital type 1 syndrome gene. *Hum Mol Genet,* 18**,** 289-303.

Fry, A. M., Meraldi, P. & Nigg, E. A. 1998. A centrosomal function for the human Nek2 protein kinase, a member of the NIMA family of cell cycle regulators. *EMBO J,* 17**,** 470-81.

Huangfu, D., Liu, A., Rakeman, A. S., Murcia, N. S., Niswander, L. & Anderson, K. V. 2003. Hedgehog signalling in the mouse requires intraflagellar transport proteins. *Nature,* 426**,** 83-7.

Kasahara, K., Kawakami, Y., Kiyono, T., Yonemura, S., Kawamura, Y., Era, S., Matsuzaki, F., Goshima, N. & Inagaki, M. 2014. Ubiquitin-proteasome system controls ciliogenesis at the initial step of axoneme extension. *Nat Commun,* 5**,** 5081.

Kim, J., Lee, J. E., Heynen-Genel, S., Suyama, E., Ono, K., Lee, K., Ideker, T., Aza-Blanc, P. & Gleeson, J. G. 2010. Functional genomic screen for modulators of ciliogenesis and cilium length. *Nature,* 464**,** 1048-51.

Kubo, A., Sasaki, H., Yuba-Kubo, A., Tsukita, S. & Shiina, N. 1999. Centriolar satellites: molecular characterization, ATP-dependent movement toward centrioles and possible involvement in ciliogenesis. *J Cell Biol,* 147**,** 969-80.

Lange, B. M. & Gull, K. 1995. A molecular marker for centriole maturation in the mammalian cell cycle. *J Cell Biol,* 130**,** 919-27.

Luxton, G. W. & Gundersen, G. G. 2011. Orientation and function of the nuclear-centrosomal axis during cell migration. *Curr Opin Cell Biol,* 23**,** 579-88.

Mogensen, M. M., Malik, A., Piel, M., Bouckson-Castaing, V. & Bornens, M. 2000. Microtubule minus-end anchorage at centrosomal and non-centrosomal sites: the role of ninein. *J Cell Sci,* 113 (Pt 17)**,** 3013-23.

Nakagawa, Y., Yamane, Y., Okanoue, T., Tsukita, S. & Tsukita, S. 2001. Outer dense fiber 2 is a widespread centrosome scaffold component preferentially associated with mother centrioles: its identification from isolated centrosomes. *Mol Biol Cell,* 12**,** 1687-97.

Nigg, E. A. & Raff, J. W. 2009. Centrioles, centrosomes, and cilia in health and disease. *Cell,* 139**,** 663-78.

Nobes, C. D. & Hall, A. 1999. Rho GTPases control polarity, protrusion, and adhesion during cell movement. *J Cell Biol,* 144**,** 1235-44.

Novorol, C., et al. 2013. Microcephaly models in the developing zebrafish retinal neuroepithelium point to an underlying defect in metaphase progression. *Open Biol,* 3**,** 130065.

Ong, A. C. & Wheatley, D. N. 2003. Polycystic kidney disease--the ciliary connection. *Lancet,* 361**,** 774-6.

Pampliega, O., et al. 2013. Functional interaction between autophagy and ciliogenesis. *Nature,* 502**,** 194-200.

Ponsard, C., Seltzer, V., Perret, E., Tournier, F. & Middendorp, S. 2007. Identification of BCAP, a new protein associated with basal bodies and centrioles. *Front Biosci,* 12**,** 3683-93.

Sambrook, J. & Russell, D. 2001. *Molecular Cloning: A Laboratory Manual,* New York, Cold Spring Harbor Laboratory Press.

Satir, P. & Christensen, S. T. 2007. Overview of structure and function of mammalian cilia. *Annu Rev Physiol,* 69**,** 377-400.

Schmidt, T. I., Kleylein-Sohn, J., Westendorf, J., Le Clech, M., Lavoie, S. B., Stierhof, Y. D. & Nigg, E. A. 2009. Control of centriole length by CPAP and CP110. *Curr Biol,* 19**,** 1005-11.

Singla, V., Romaguera-Ros, M., Garcia-Verdugo, J. M. & Reiter, J. F. 2010. Ofd1, a human disease gene, regulates the length and distal structure of centrioles. *Dev Cell,* 18**,** 410-24.

Sorokin, S. 1962. Centrioles and the formation of rudimentary cilia by fibroblasts and smooth muscle cells. *J Cell Biol,* 15**,** 363-77.

Stevens, N. R., Raposo, A. A., Basto, R., St Johnston, D. & Raff, J. W. 2007. From stem cell to embryo without centrioles. *Curr Biol,* 17**,** 1498-503.

Stowe, T. R., Wilkinson, C. J., Iqbal, A. & Stearns, T. 2012. The centriolar satellite proteins Cep72 and Cep290 interact and are required for recruitment of BBS proteins to the cilium. *Mol Biol Cell,* 23**,** 3322-35.

Tang, Z., Lin, M. G., Stowe, T. R., Chen, S., Zhu, M., Stearns, T., Franco, B. & Zhong, Q. 2013. Autophagy promotes primary ciliogenesis by removing OFD1 from centriolar satellites. *Nature,* 502**,** 254-7.

Tassin, A. M. & Bornens, M. 1999. Centrosome structure and microtubule nucleation in animal cells. *Biol Cell,* 91**,** 343-54.

Tollenaere, M. A., Mailand, N. & Bekker-Jensen, S. 2015. Centriolar satellites: key mediators of centrosome functions. *Cell Mol Life Sci,* 72**,** 11-23.

Tsang, W. Y., Bossard, C., Khanna, H., Peranen, J., Swaroop, A., Malhotra, V. & Dynlacht, B. D. 2008. CP110 suppresses primary cilia formation through its interaction with CEP290, a protein deficient in human ciliary disease. *Dev Cell,* 15**,** 187-97.

Uetake, Y. & Sluder, G. 2007. Cell-cycle progression without an intact microtuble cytoskeleton. *Curr Biol,* 17**,** 2081-6.

Vladar, E. K. & Stearns, T. 2007. Molecular characterization of centriole assembly in ciliated epithelial cells. *J Cell Biol,* 178**,** 31-42.

Wells, C. M. & Parsons, M. 2011. *Cell migration : developmental methods and protocols,* New York, Humana Press ; Springer.

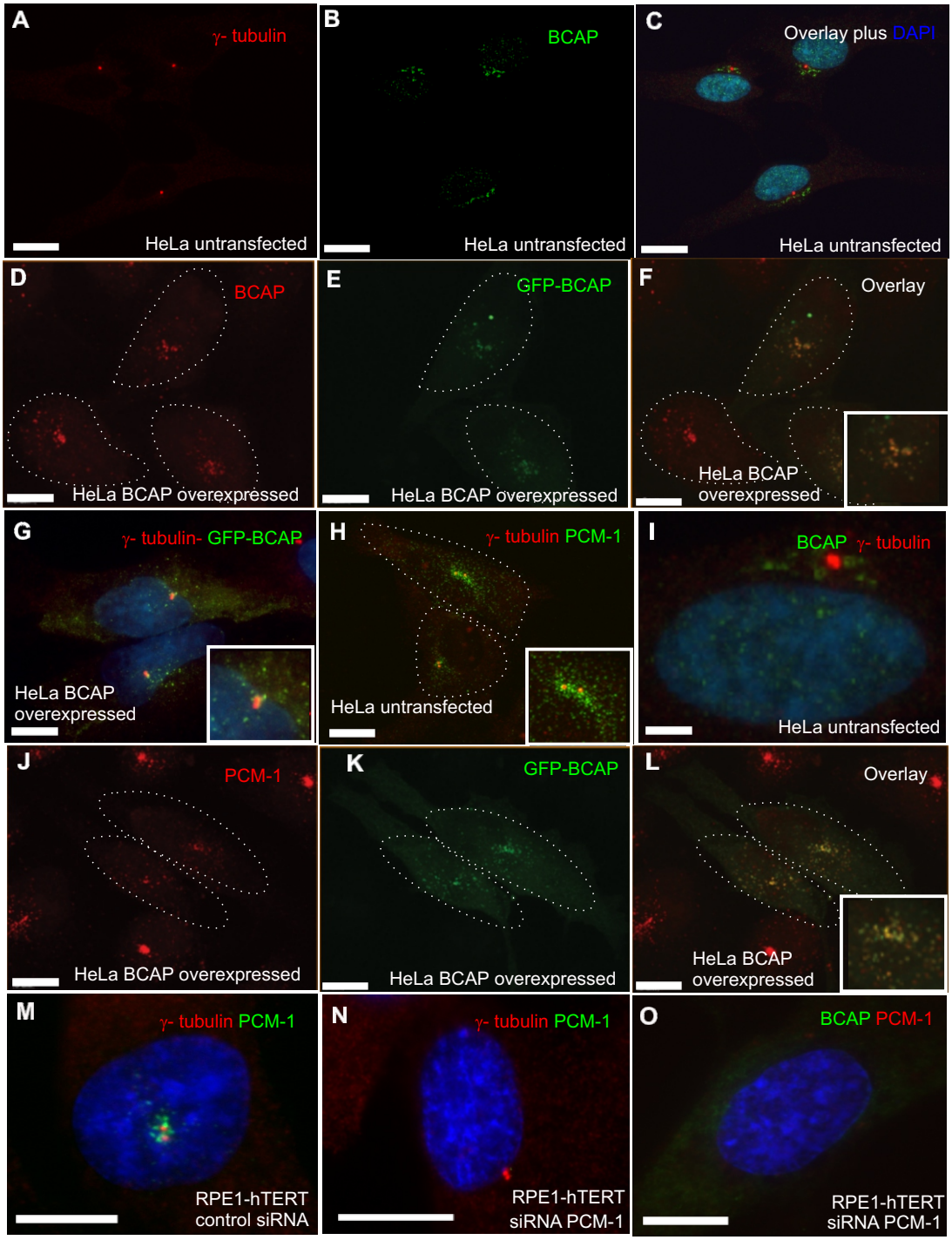
A
γ- tubulin
HeLa untransfected
B
BCAP
HeLa untransfected
C
Overlay plus DAPI
HeLa untransfected
D
BCAP
HeLa BCAP overexpressed
E
GFP-BCAP
HeLa BCAP overexpressed
F
Overlay
HeLa BCAP
overexpressed
G
γ- tubulin- GFP-BCAP
HeLa BCAP
overexpressed
H
γ- tubulin PCM-1
HeLa untransfected
I
BCAP γ- tubulin
HeLa untransfected
J
PCM-1
HeLa BCAP overexpressed
K
GFP-BCAP
HeLa BCAP overexpressed
L
Overlay
HeLa BCAP
overexpressed
M
γ- tubulin PCM-1
RPE1-hTERT
control siRNA
N
γ- tubulin PCM-1
RPE1-hTERT
siRNA PCM-1
O
BCAP PCM-1
RPE1-hTERT
siRNA PCM-1

Figure 1

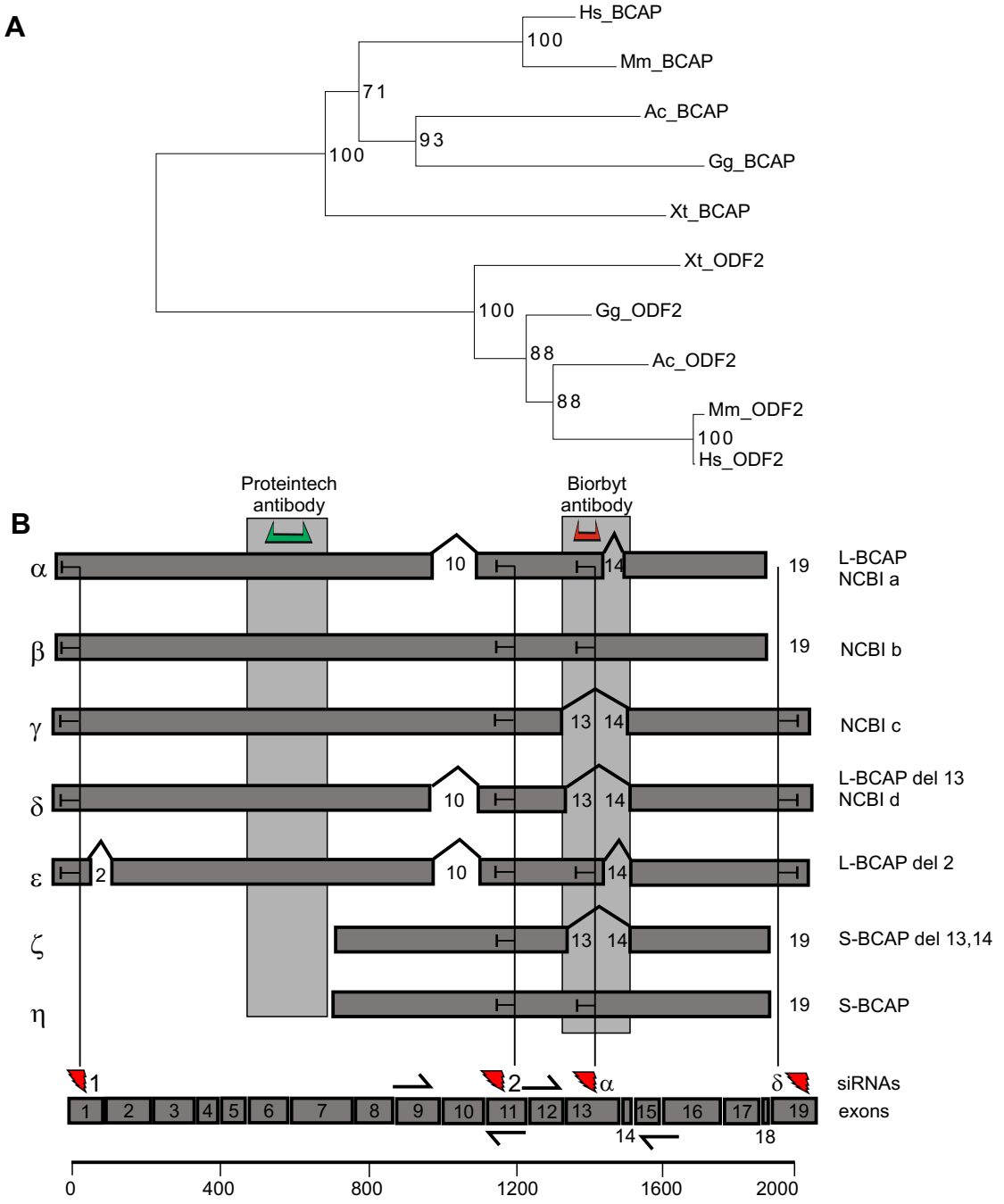
A
Hs_BCAP
100
Mm_BCAP
71
Ac_BCAP
93
Gg_BCAP
100
Xt_BCAP
Xt_ODF2
100
Gg_ODF2
88
Ac_ODF2
88
Mm_ODF2
100
Hs_ODF2
B
Proteintech antibody
Biorbyt antibody
α
β
γ
δ
ε
ζ
η
L-BCAP NCBI a
NCBI b
NCBI c
L-BCAP del 13 NCBI d
L-BCAP del 2
S-BCAP del 13,14
S-BCAP
siRNAs
exons
0
400
800
1200
1600
2000

Figure 2

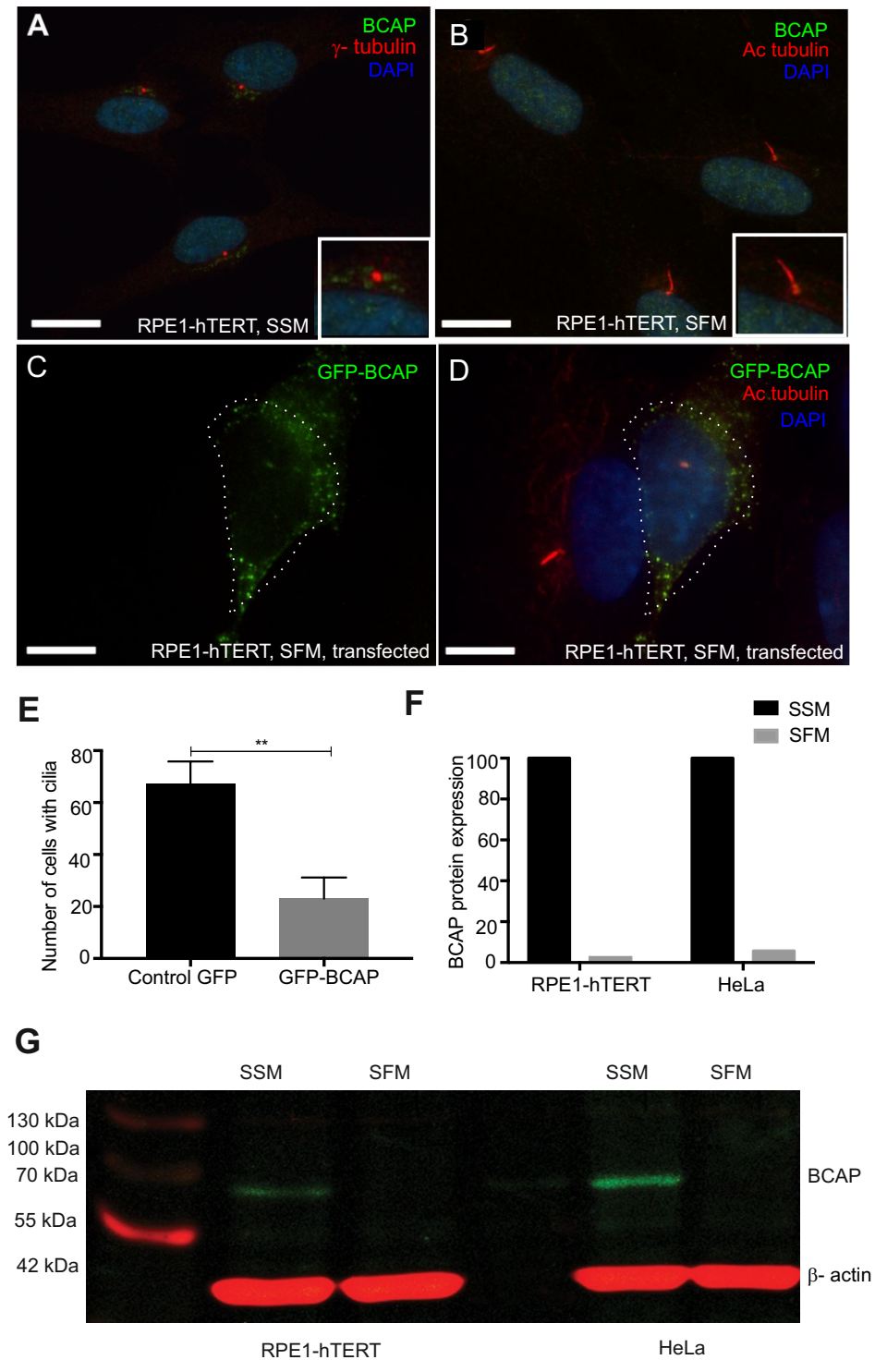
A
BCAP
γ- tubulin
DAPI
RPE1-hTERT, SSM
B
BCAP
Ac tubulin
DAPI
RPE1-hTERT, SFM
C
GFP-BCAP
RPE1-hTERT, SFM, transfected
D
GFP-BCAP
Ac tubulin
DAPI
RPE1-hTERT, SFM, transfected
E
Number of cells with cilia
80
60
40
20
0
**
Control GFP
GFP-BCAP
F
SSM
SFM
BCAP protein expression
100
80
60
40
20
0
RPE1-hTERT
HeLa
G
SSM
SFM
SSM
SFM
130 kDa
100 kDa
70 kDa
55 kDa
42 kDa
BCAP
β- actin
RPE1-hTERT
HeLa

Figure 3

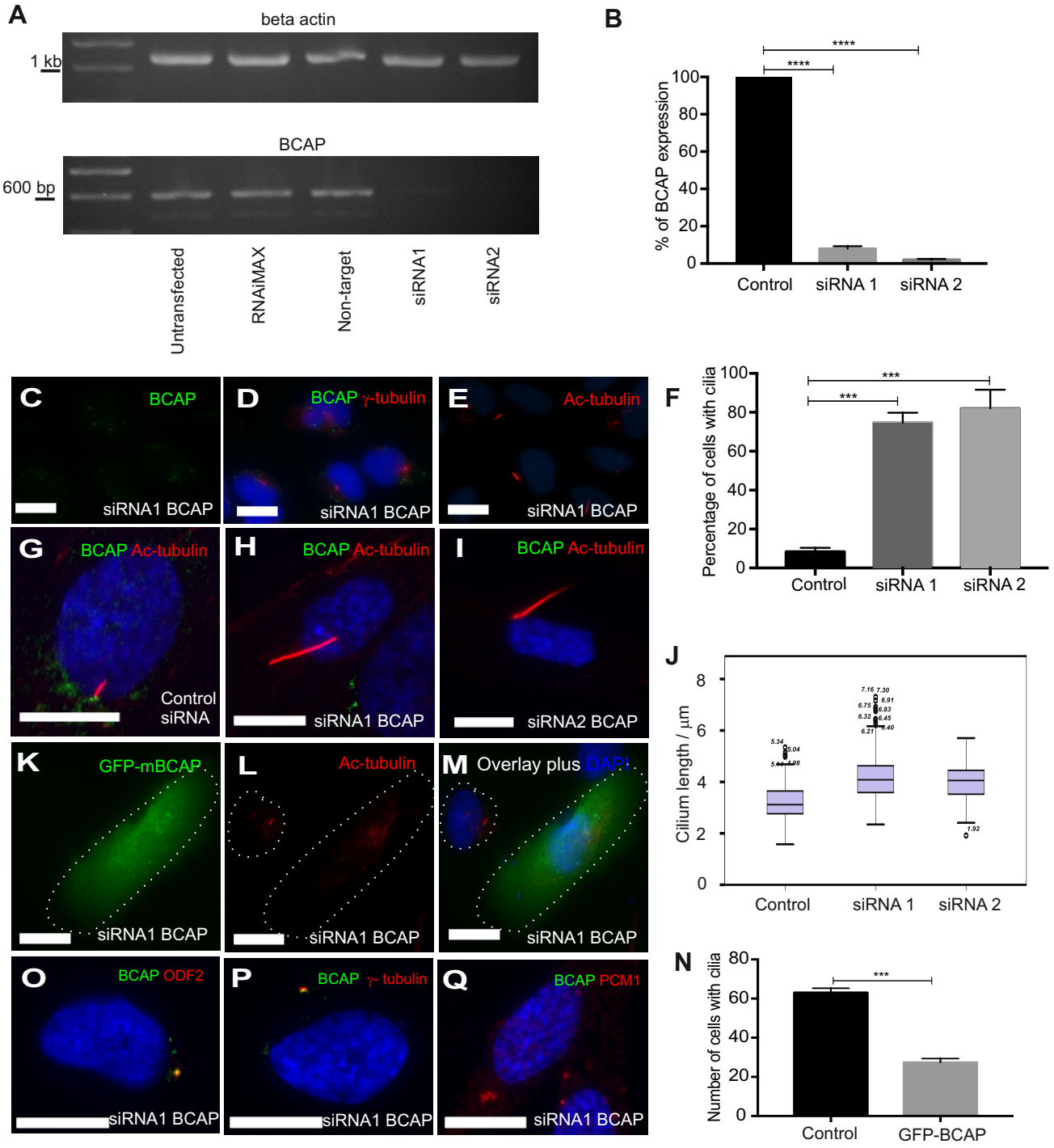
A
beta actin
1 kb
BCAP
600 bp
Untransfected
RNAiMAX
Non-target
siRNA1
siRNA2
B
% of BCAP expression
Control
siRNA 1
siRNA 2
C BCAP siRNA1 BCAP
D BCAP γ-tubulin siRNA1 BCAP
E Ac-tubulin siRNA1 BCAP
F
Percentage of cells with cilia
Control
siRNA 1
siRNA 2
G BCAP Ac-tubulin Control siRNA
H BCAP Ac-tubulin siRNA1 BCAP
I BCAP Ac-tubulin siRNA2 BCAP
J
Cilium length / µm
Control
siRNA 1
siRNA 2
K GFP-mBCAP siRNA1 BCAP
L Ac-tubulin siRNA1 BCAP
M Overlay plus DAPI siRNA1 BCAP
N
Number of cells with cilia
Control
GFP-BCAP
O BCAP ODF2 siRNA1 BCAP
P BCAP γ- tubulin siRNA1 BCAP
Q BCAP PCM1 siRNA1 BCAP

Figure 4

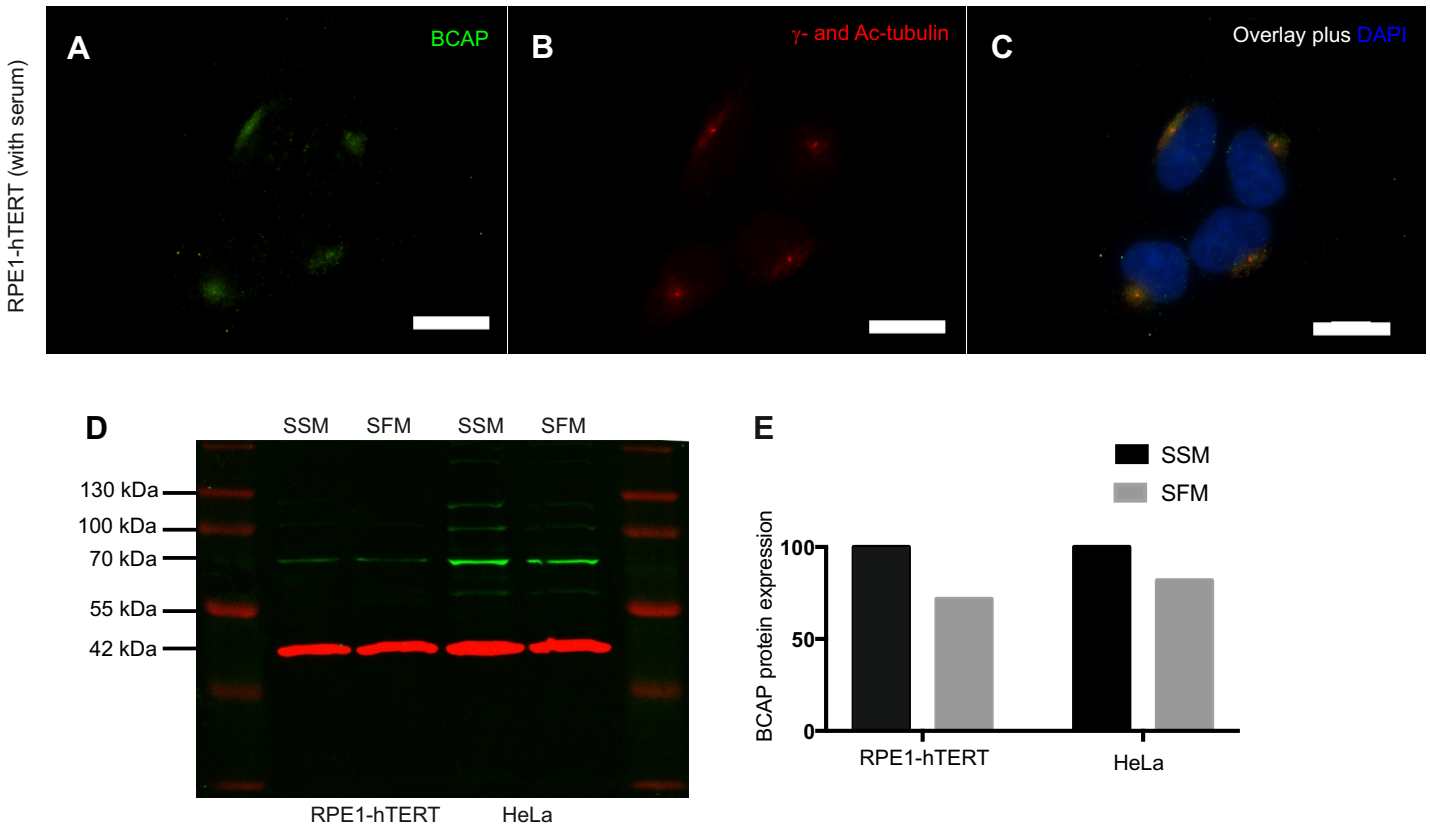
RPE1-hTERT (with serum)
A
BCAP
B
γ- and Ac-tubulin
C
Overlay plus DAPI
D
SSM
SFM
SSM
SFM
130 kDa
100 kDa
70 kDa
55 kDa
42 kDa
RPE1-hTERT
HeLa
E
SSM
SFM
BCAP protein expression
100
50
0
RPE1-hTERT
HeLa

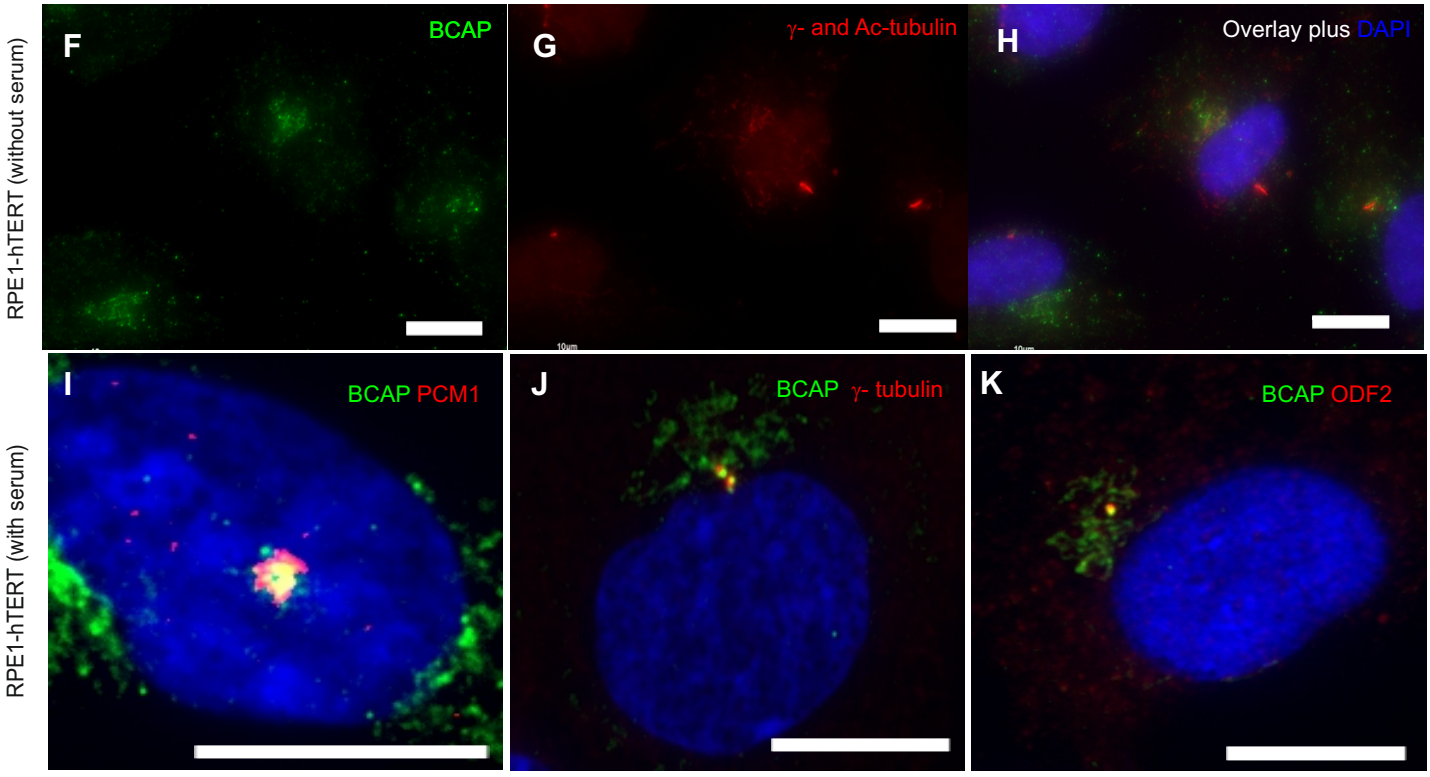
RPE1-hTERT (without serum)
F
BCAP
G
γ- and Ac-tubulin
H
Overlay plus DAPI
RPE1-hTERT (with serum)
I
BCAP PCM1
J
BCAP γ- tubulin
K
BCAP ODF2

Figure 5

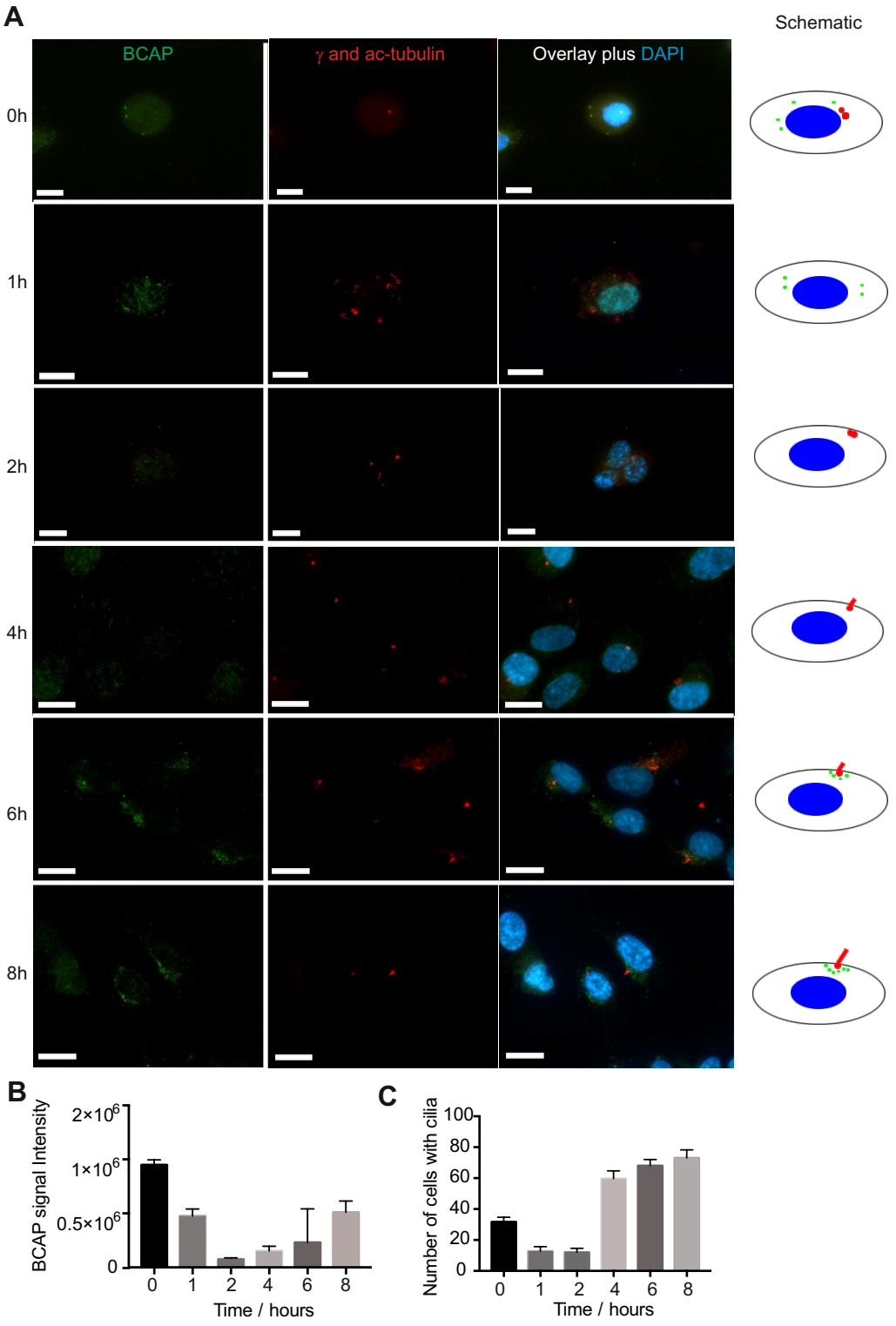
A
BCAP
γ and ac-tubulin
Overlay plus DAPI
Schematic
0h
1h
2h
4h
6h
8h
B
BCAP signal Intensity
2×10^6
1×10^6
0.5×10^6
0
0 1 2 4 6 8
Time / hours
C
Number of cells with cilia
100
80
60
40
20
0
0 1 2 4 6 8
Time / hours

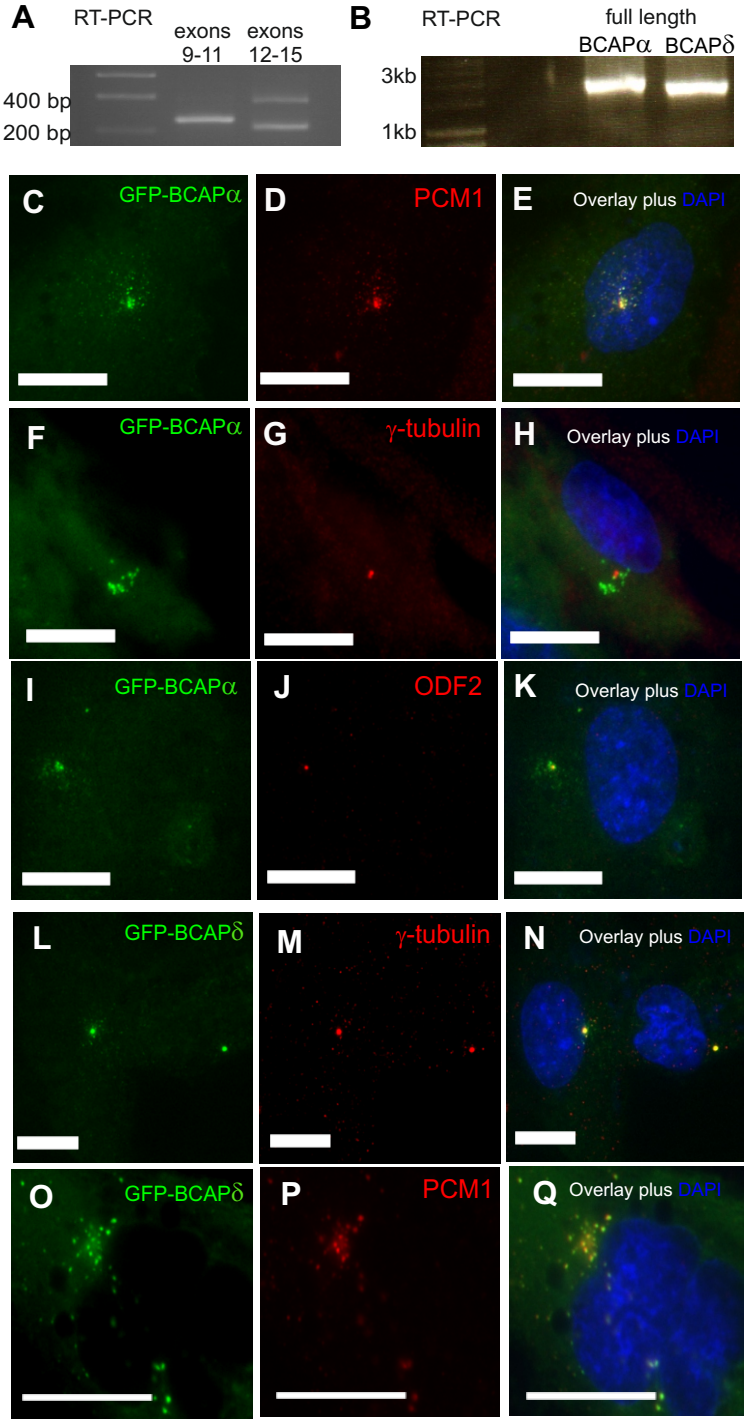
A
RT-PCR
exons 9-11
exons 12-15
400 bp
200 bp
B
RT-PCR
full length
BCAPα
BCAPδ
3kb
1kb
C
GFP-BCAPα
D
PCM1
E
Overlay plus DAPI
F
GFP-BCAPα
G
γ-tubulin
H
Overlay plus DAPI
I
GFP-BCAPα
J
ODF2
K
Overlay plus DAPI
L
GFP-BCAPδ
M
γ-tubulin
N
Overlay plus DAPI
O
GFP-BCAPδ
P
PCM1
Q
Overlay plus DAPI

Figure 7

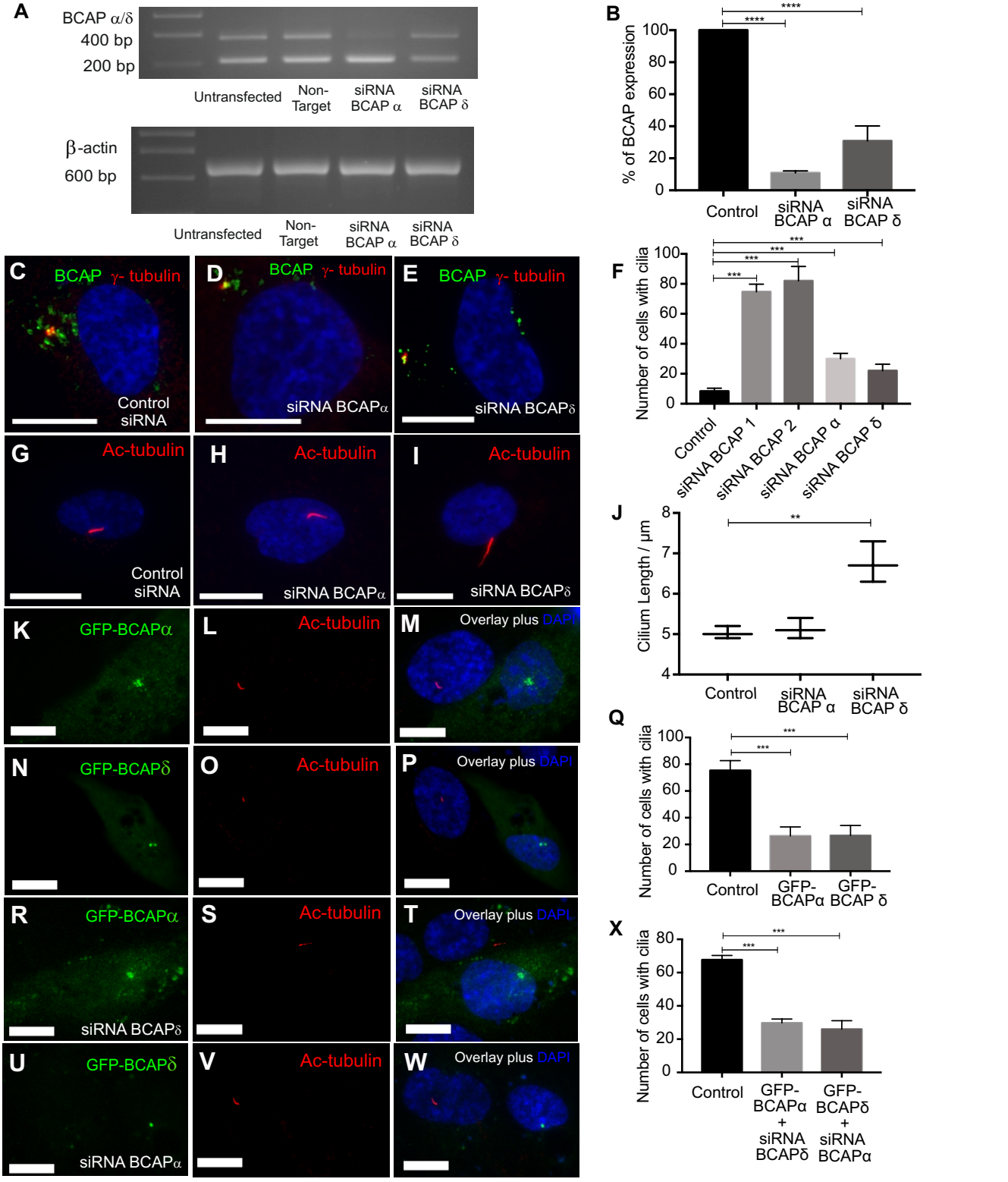
A
BCAP α/δ
400 bp
200 bp
Untransfected
Non-Target
siRNA BCAP α
siRNA BCAP δ
β-actin
600 bp
Untransfected
Non-Target
siRNA BCAP α
siRNA BCAP δ
B
% of BCAP expression
Control
siRNA BCAP α
siRNA BCAP δ
C
BCAP γ- tubulin
Control siRNA
D
BCAP γ- tubulin
siRNA BCAPα
E
BCAP γ- tubulin
siRNA BCAPδ
F
Number of cells with cilia
Control
siRNA BCAP 1
siRNA BCAP 2
siRNA BCAP α
siRNA BCAP δ
G
Ac-tubulin
Control siRNA
H
Ac-tubulin
siRNA BCAPα
I
Ac-tubulin
siRNA BCAPδ
J
Cilium Length / µm
Control
siRNA BCAP α
siRNA BCAP δ
K
GFP-BCAPα
L
Ac-tubulin
M
Overlay plus DAPI
N
GFP-BCAPδ
O
Ac-tubulin
P
Overlay plus DAPI
Q
Number of cells with cilia
Control
GFP-BCAPα
GFP-BCAP δ
R
GFP-BCAPα
siRNA BCAPδ
S
Ac-tubulin
T
Overlay plus DAPI
U
GFP-BCAPδ
siRNA BCAPα
V
Ac-tubulin
W
Overlay plus DAPI
X
Number of cells with cilia
Control
GFP-BCAPα + siRNA BCAPδ
GFP-BCAPδ + siRNA BCAPα